

Nonequilibrium Fluctuations in a Gaussian Galton Board (or Periodic Lorentz Gas) Using Long Periodic Orbits

Wm. G. Hoover and Carol G. Hoover

Ruby Valley Research Institute

Highway Contract 60, Box 601

Ruby Valley, Nevada 89833

(Dated: June 20, 2018)

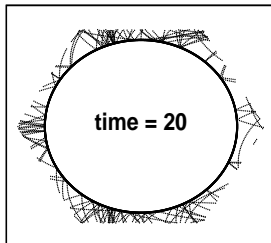
Abstract

Predicting nonequilibrium fluctuations requires a knowledge of nonequilibrium distribution functions. Despite the distributions' fractal character some theoretical results, "Fluctuation Theorems", reminiscent of but distinct from, Gibbs' equilibrium statistical mechanics and the Central Limit Theorem, have been established away from equilibrium and applied to simple models. We summarize the simplest of these results for a Gaussian-thermostated Galton Board problem, a field-driven mass point moving through a periodic array of hard-disk scatterers. The billion-collision trillion-timestep data we analyze correspond to periodic orbits with up to 793,951,594 collisions and 447,064,397,614 timesteps.

PACS numbers: 05.45.Df, 05.45.Pq, 74.40.Gh, 05.70.Ln

Keywords: Galton Board, Lyapunov Spectrum, Fluctuations, Nonequilibrium

Figure 1



$$-0.7 < x \text{ and } y < +0.7$$

FIG. 1: A periodic hexagonal unit cell description of the thermostated Galton Board. A point particle is scattered by the disk of unit diameter at the cell center. The scatterer density is $4/5$ the close-packed density, so that the center-to-center spacing of the scatterers is $\sqrt{5/4}$. The accelerating field, $E = 3$, is directed toward the right, in the horizontal x direction. The preponderance of collisions at the lefthandside of the scatterer reflects the resulting positive current, which has a mean value $\langle p_x \rangle = 0.220$. The magnitude of the velocity is unity so that the instantaneous current always lies between -1 and $+1$. Accordingly, the time-averaged entropy production rate is $\langle \sigma \rangle / k = \langle \dot{S} \rangle / k = E \langle p_x \rangle / kT = 0.660$. The combined length of the trajectory segments shown in the Figure, 20, is equal to the elapsed time. A coarse-grained (twelve-digit) description of the model with a fourth-order Runge-Kutta timestep $dt = 0.0005$ results in a 793,951,594-collision periodic-orbit problem as is discussed in the text.

I. INTRODUCTION

In preparing a second edition of *Time Reversibility, Computer Simulation, and Chaos*¹ we are presently summarizing some of the recent work in this field in a pedagogical form. We would appreciate readers' suggestions as to topics which ought to be included or expanded. One such topic is considered here, "Fluctuation Theorems".

By now there is a voluminous literature devoted to Fluctuation Theorems of the type described first in 1993 by Evans, Cohen, and Morriss^{2,3}. These theorems relate the relative probabilities of sufficiently-long forward and reversed nonequilibrium trajectory segments to the corresponding external entropy produced along the forward trajectory²⁻⁶. The time-reversibility of deterministic thermostated motion equations simplifies such calculations.

Among the simplest applications is the "Galton Board" problem, the field-driven motion

of a point particle through a periodic array of hard-disk scatterers^{7,8}. We illustrate that application here as a worked-out pedagogical exercise problem. This problem makes contact with other areas of the research literature: periodic orbit analysis⁹⁻¹³ and the effects of finite precision on simulation results^{9,10}. We simplify the analysis by considering a phase-space distribution representing a single periodic orbit. The orbit is long enough (millions of collisions and billions of timesteps) to closely approximate a full nonequilibrium ensemble average. The orbit lengths used appear in Table I. They are sensitive to the exact details of the trajectory calculation. Related examples of the underlying Galton Board problem have been discussed at length in the literature^{4-6,13,14}.

Table I. Number of decimal digits n , number of collisions, number of timesteps, and collision rate Γ in typical periodic orbits where each collision is centered in a phase-space cell described with a spacing of n decimal digits. The fourth-order Runge-Kutta timestep is 0.0005. The correlation dimension $D_2 = 1.583$ from Reference 19 predicts orbit lengths of order $10^{0.79n} \simeq 3 \times 10^9$ for $n = 12$.

n	collisions	timesteps	Γ
3	774	440 812	3.512
4	10 175	5 794 556	3.512
5	5 133	2 886 067	3.557
6	53 042	29 911 691	3.547
7	77 418	43 668 154	3.546
8	5 004 959	2 819 006 271	3.551
9	2 946 042	1 660 446 602	3.548
10	18 398 545	10 359 262 120	3.552
11	85 030 972	47 885 512 832	3.551
12	793 951 594	447 064 397 614	3.552

Figure 2

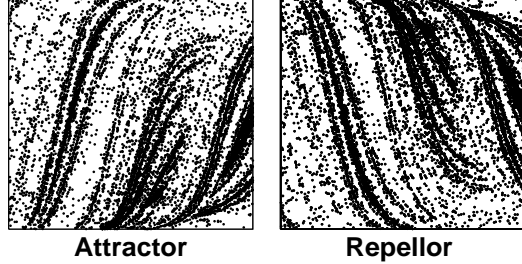


FIG. 2: 10 175-point periodic attractor and the corresponding (mirror-image) repellor, using four decimal digits to divide the collision space shown into $10^4 \times 10^4 = 10^8$ separate states. The abscissa is $0 < \alpha < \pi$ and the ordinate is $-1 < \sin(\beta) < +1$; α gives the location of a collision relative to the field direction, while β gives the angle between the post-collision velocity vector and the outward normal vector at the collision location. Reversing the time corresponds to changing the sign of the ordinate.

II. BACKGROUND

Consider the longtime phase-space probability density $f(q, p, \zeta)$ generated by motion in a nonequilibrium steady state. Besides the details of the time-dependent coordinates $\{q\}$ and momenta $\{p\}$, included also is at least one thermostat variable ζ , which defines the external time-dependent entropy production rate $\sigma = \dot{S}$ required to maintain the steady state. When Nosé-Hoover thermostats are used the friction coefficient(s) $\{\zeta\}$ are independent variables, obeying their own differential equations:

$$\{ F_{\text{NH}} \equiv -\zeta p \} ; \{ \dot{\zeta} \propto \sum [(p^2/mkT) - 1] \} .$$

and guaranteeing that the thermostated momenta included in the sum(s) have longtime average kinetic temperature(s) $\{T\}$.

In the one-body Galton Board simulation problem analyzed in Sections III and IV ζ is not an independent variable, but is instead an explicit linear function of the momentum, a ‘‘Gaussian thermostat’’, keeping the kinetic temperature constant:

$$F_{\text{G}} \equiv -\zeta p ; \zeta = \zeta(p) \propto p_x \longrightarrow p^2 \equiv mkT.$$

To simplify our analysis we consider here computational models “solved” by generating finite-difference approximations to their system trajectories. Finite-difference schemes in bounded phase spaces eventually begin to repeat their history. Estimating the number of steps both prior to and during the repetition is analogous to solving the “Birthday Problem”, “How large must a randomly-chosen group of people be to make it likely that two share the same birthday?”. Similarly, random jumps in an N -state phase space suggest a longest periodic orbit length of order \sqrt{N} jumps, a second-longest orbit shorter by a factor of e , a third-longest orbit shorter by e^2 , and so on. Thus in practice there are only a few ($\simeq \ln \sqrt{N}$) *periodic orbits* in a finite-precision phase space^{9,10} with their combined lengths less than twice that of the longest periodic orbit. In a *nonequilibrium* situation, with a multifractal attractor having a reduced phase-space dimensionality, there are even-fewer, even-shorter paths. The details can be expressed in terms of the multifractal distribution’s “correlation dimension”, which gives the dimensionality of nearby pairs of trajectory points^{9,10}.

By considering only the longest most-likely of these numerical orbits, the resulting “natural measure” in the space is a constant, $f = 1/\Omega$ at each of the Ω discrete points of the orbit and is zero elsewhere in the space. In a typical nonequilibrium steady state the length of this longest single orbit exceeds the combined lengths of all the rest in the fine-mesh limit^{9,10}. With double-precision arithmetic the typical mesh size is of order 10^{-14} .

All of the longest-orbit system variables, including σ the rate of external entropy production due to the thermostat, are necessarily periodic functions of time with period τ , the orbit length. The external entropy produced per period is a positive constant, $\tau\langle\sigma\rangle$. Because the nonequilibrium motion equations underlying our continuous-time problem are all *time-reversible*, we can also usefully imagine a highly-improbable time-reversed *backward* version of the periodic orbit. See Figure 2 for a four-digit example. This “repellor” trajectory, the time-reversed attractor, is a bit artificial. It can be generated in either of two fully-equivalent ways: [1] solve the differential equations for $\{q, p, \zeta\}$ as usual, but with a *negative timestep* $dt \rightarrow -dt$ or [2] take the stored solution of the equations with a positive dt and change the signs of the $\{p\}$ and $\{\zeta\}$. Because a finite bounded phase-space distribution requires that the Lyapunov instability^{12,13} of the reversed orbit necessarily exceeds that of the forward attractor, the reversed orbit can only be generated in the two ways just mentioned.

Fluctuation Theorems describe the *relative probability* of finite-but-large *segments* of such forward-backward pairs. Unlike the Central Limit Theorem, which predicts the longtime

(Gaussian) *shape* of the probability distribution, the Fluctuation Theorems instead predict ratios of forward/backward probabilities. By considering the simplest computational case where the phase-space motion is periodic, but dissipative, the discussion of this single-orbit problem avoids the need to address ergodicity as well as sign changes in the values of the local (coordinate-dependent) Lyapunov exponents.

Consider an observation time $\delta\tau$ (perhaps as small as a single timestep and possibly as large as the total length τ of the periodic orbit under consideration). Averaging the location of the observation time over the entire orbit gives exactly the same rate of external entropy production (due to the thermostat) as characterizes the full orbit:

$$\langle\sigma\rangle_{\delta\tau} = (1/\delta\tau)\Delta S_{\delta\tau} \equiv (1/\tau)\Delta S_{\tau} = \langle\sigma\rangle_{\tau} = (1/\tau)(work/T)_{\text{orbit}} = (1/\tau)(heat/T)_{\text{orbit}} .$$

The *work* done (by a driving external field), summed up over the entire orbit, is necessarily equal to the total *heat* extracted by the constant-temperature thermostat. Dividing by the thermostat temperature T gives the corresponding entropy produced, $\Delta S = (heat/T)_{\text{orbit}}$. In the special case we consider in Sections III and IV the kinetic temperature is fixed by using a ‘‘Gaussian’’ thermostat. Gauss’ *Principle of Least Constraint* provides a basis for this approach. The Principle suggests using the smallest possible rms force to constrain the kinetic temperature T . This ‘‘least’’ force is linear in the momentum. We define the kinetic temperature T in the usual way: $T = p^2/mk = 1$. Fluctuation Theorems with fluctuating temperatures and with stochastic thermostats have also been considered and tested^{4-6,15}.

The relative probabilities of the forward ‘‘attractor’’ and reversed ‘‘repellor’’ orbits (if we now imagine them as the two infrequently communicating parts of an ergodic steady continuous distribution) can be expressed in terms of their orbit-averaged Lyapunov exponents. The entire spectrum of Lyapunov exponents, both positive and negative, can be determined using a finite-difference algorithm, as described by Bennetin¹⁶, or by using continuous-time Lagrange multiplier constraints^{17,18}. The positive exponents, which describe spreading, can be used to express the loss rate of probability density from the neighborhoods of the forward and backward orbits. These loss rates for the attractor A and repellor R must balance in a steady state. Averaged over a single periodic orbit, this balance expresses the attractor and repellor probabilities in terms of the dissipation induced by the thermostat:

$$f_A \exp\left[\sum_{\lambda_A>0} -\lambda_A\tau\right] = f_R \exp\left[\sum_{\lambda_R>0} -\lambda_R\tau\right] \longleftrightarrow \frac{f_A}{f_R} = \frac{e^{\sum\lambda_A\tau}}{e^{-\sum\lambda_R\tau}} = e^{\langle\dot{S}\rangle\tau/k} .$$

Because the positive exponents on the repeller are simply reversed-sign versions of the negative exponents on the attractor the two Lyapunov-exponent sums can be combined:

$$\ln \left[\frac{f_{\text{forward}}}{f_{\text{backward}}} \right] = \ln \left[\frac{f_A}{f_R} \right] = \sum_{\lambda_A > 0} \lambda_A \tau - \sum_{\lambda_R > 0} \lambda_R \tau \equiv \sum_A \lambda \tau = \langle \dot{S} \rangle \tau / k . \quad [FT]$$

The usual statement of this Fluctuation Theorem [FT] includes the proviso that the averaging time τ must be sufficiently large. It is evident that the steady state quotient f_A/f_R is typically positive, as the Second Law states, so that the longtime expression [FT] fails as τ approaches zero.

For Gauss' or Nosé-Hoover thermostats the equality between the complete sum of all the local Lyapunov exponents and the external rate of entropy production is an identity. For the Galton Board example which we detail in Section III this equality follows directly from an application of Liouville's Theorem to the nonHamiltonian equations of motion suggested by Gauss' Principle.

The Fluctuation Theorem illustrated here was first demonstrated, numerically, for a manybody shear flow². We illustrate the same Theorem in the next Section for a simple pedagogical example, the thermostated one-particle Galton Board^{1,4,6-8,10,13,14,19,20}. We divide up a single relatively-long finite-precision periodic orbit into portions $\delta\tau$. Evidently the overall averaged dissipation rate for these portions is the same as the rate for the entire orbit $\langle \sigma \rangle_\tau$ so that we can test the applicability of the Theorem as a function of the sampling time $\delta\tau$.

III. GALTON BOARD

The Galton Board problem provides an instructive example of all these ideas. A point particle with unit mass is accelerated to the right by a field E through a triangular lattice of fixed disk scatterers. For this problem the average current $\langle p_x \rangle$, dissipated energy, and entropy production are all simply related:

$$p^2 \equiv kT \equiv 1 \longleftrightarrow E \langle p_x \rangle = \langle (d/dt)work \rangle = \langle (d/dt)heat \rangle = \langle \zeta p^2 \rangle .$$

The speed $|p/m|$ of the point particle, as well as its "temperature" p^2/mk , is kept constant by the friction coefficient $\zeta = Ep_x/p^2$:

$$\zeta = (d/dt)work/kT = (d/dt)heat/kT = \dot{S}/k .$$

Here $\dot{S} = \sigma$ is the instantaneous external entropy production rate. The complete set of motion equations for the isokinetic Galton Board is the following:

$$\dot{x} = p_x ; \dot{y} = p_y ; \dot{p}_x = F_x + E - \zeta p_x ; \dot{p}_y = F_y - \zeta p_y .$$

By switching to polar momentum coordinates these trajectory equations can be integrated analytically⁷, though here we choose to use the equally accurate (machine accuracy) fourth-order Runge-Kutta integration for simplicity's sake. The hard-disk elastic force F is the reflective interaction of the point particle and the fixed scatterer, where the collision location and direction are given by the angles $\{\alpha, \beta\}$ defined in the caption of Figure 2. The collisional “jumps” in the phase-space orbit contribute to the Lyapunov instability of the problem, but make no contribution to the work done by the field or to the heat extracted by the thermostat and converted to external entropy production. In the numerical work the coordinates and momenta are rescaled (with m, k , and the scatterer diameter all equal to unity),

$$x^2 + y^2 \longrightarrow 0.25 ; p_x^2 + p_y^2 \longrightarrow 1 ,$$

whenever the accurate Runge-Kutta trajectory returns $\{x, y\}$ values inside the scatterer radius of 1/2.

We apply this model to the Fluctuation Theorem by considering the situation indicated in Figure 1 for a periodic unit cell. The Figure shows an illustrative trajectory portion made up of 20 000 timesteps, with $dt = 0.001$. In the equilibrium case, with zero field, the scatterer collisions make all velocity directions equally probable so that the probability density for $p_x = \cos(\theta)$ diverges at ± 1 :

$$\begin{aligned} \frac{d\theta}{2\pi} &= \text{prob}(\theta)d\theta = \text{prob}(p_x)dp_x \rightarrow \\ \text{prob}(p_x) &= \frac{(|d\theta/dp_x|)}{2\pi} = \frac{1}{2\pi|\sin(\theta)|} = \frac{1}{2\pi\sqrt{1-p_x^2}} = \frac{1}{2\pi|p_y|} . \end{aligned}$$

With the field turned “on” the downhill directions become more probable, as is illustrated by the trajectory segment of Figure 1 and by the two probability densities, normalized for 400 momentum bins, shown in Figure 3. With the field “off”, and all velocity directions equally likely the probability density for p_x diverges at the extrema, $p_x = \pm 1$.

The low-field dynamics is Lyapunov unstable²⁰, with two nonzero Lyapunov exponents, $\{\lambda\} = \{\pm 3.922\}$ at zero field, and $\{\lambda\} = \{3.000 ; -3.658\}$ with a field strength of $E = 3.00$.

Figure 3

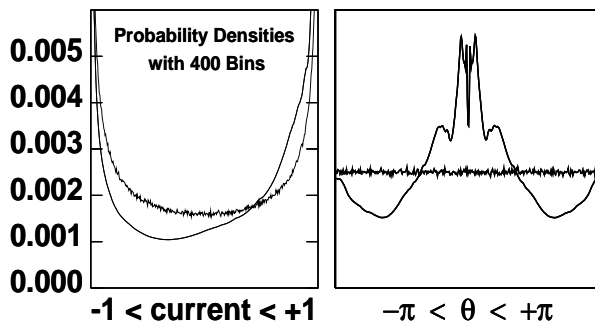


FIG. 3: 400-bin probability distributions for the current and for the direction of the velocity, varying from parallel to antiparallel, $\theta = \arctan(p_y/p_x)$ for no field (jagged symmetric data) and for a field strength of 3.00. The relatively complex peak at $\theta = 0$ corresponds to the enhanced probability on the lefthandside of the scatterer in Figure 1. A timestep of 0.0005 with 100 billion timesteps was used in accumulating these data.

These data for the Galton Board, and many others, for simple models and for manybody systems, are available in Christoph Dellago's 1995 Dissertation²⁰.

If the field strength is large enough, short periodic orbits with both exponents negative (20 collisions for $E = 3.69$ and 2 collisions for $E = 4.00$) can be stabilized in the infinitesimal-mesh limit. See Figures 2 and 5 of Reference 7. To avoid such nonergodic situations we choose a field strength $E = 3.00$, for which the conductivity (current divided by field) is 0.0734, significantly reduced from the lowfield¹⁴ Green-Kubo value of 0.10, and corresponding to a current $0.0734E$

$$\langle p_x \rangle = p \langle \cos(\theta) \rangle = 0.0734 \times 3 = 0.220 ,$$

and a mean squared current of 0.574. These latter numerical results were obtained in 1987⁷.

The probability densities for four different sampling times are shown in Figure 4. The longest time shown corresponds to approximately 178 collision times, while the shortest is about 1/6 of a collision time. Let us turn to the analysis of the sampling-time dependence of these results from the longtime standpoints of the Fluctuation Theorem and the Central Limit Theorem.

IV. THE FLUCTUATION AND CENTRAL LIMIT THEOREMS

The ‘‘Fluctuation Theorem’’ expresses the ratios of probabilities of forward and reversed processes, but not their shapes, ending up with expressions like this:

$$\ln \left[\frac{\text{prob}_f(+\sigma)}{\text{prob}_b(-\sigma)} \right]_{\delta\tau} = \frac{+\sigma\delta\tau}{k} ,$$

valid in the limit that $\delta\tau$ is sufficiently large. The Central Limit Theorem, also valid for large $\delta\tau$, can be expressed similarly:

$$\ln \left[\frac{\text{prob}_f(+\sigma)}{\text{prob}_b(-\sigma)} \right]_{\delta\tau} = -\frac{(+\sigma - \langle\sigma\rangle)^2}{2\Sigma^2} + \frac{(-\sigma - \langle\sigma\rangle)^2}{2\Sigma^2} = +\frac{2\sigma\langle\sigma\rangle}{\Sigma^2} ,$$

where the average entropy production here is $\langle\sigma\rangle = 0.22E = 0.66$ and Σ is the ‘‘standard deviation’’ of the Gaussian. Equating the two expressions (Fluctuation Theorem and Central Limit Theorem) gives an explicit large- $\delta\tau$ expression for Σ :

$$\Sigma = \sqrt{2k\langle\sigma\rangle/\delta\tau} .$$

A visual inspection of the current probabilities for a relatively large time averaging interval $\delta\tau = 50$ (nearly 200 collisions) reveals noticeable deviations from a smooth Gaussian shape. Much larger intervals are not practical because the probability of observing negative currents becomes small. For example, for a time interval of $\delta\tau = 100$, where we never observed a ‘‘negative entropy production’’ in our Table I sample length of $2.2 \times 10^6 \delta\tau$, the probability of the zero-current Gaussian relative to its maximum (at an entropy production rate of 0.66) is

$$\exp[-0.66^2/2\Sigma^2] = \exp[-(0.66/4) \times 100] = \exp[-16.5] \simeq 7 \times 10^{-8} .$$

For this example problem it is evident that the two longtime relations are only semiquantitative (with errors of a few percent) and don’t give the detailed shape of the probability distribution. To illustrate the Fluctuation Theorem relationship in the usual way we plot the (logarithm of the) probability ratio for a range of sampling times, from $2000dt$ to $10^5 dt$. The data shown in Figures 5 and 6, all for a single typical 12-digit periodic orbit, demonstrate that the Fluctuation Theorem, like the Central Limit Theorem, is indeed a useful semiquantitative guide provided that the sampling time is more than a few collisions and that the entropy production rate is not too large.

Figure 4

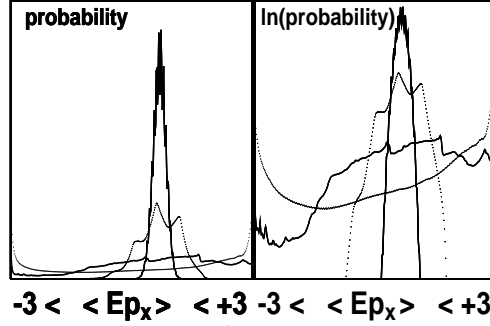


FIG. 4: Entropy production rate averaged over averaging time intervals $\delta\tau = \{50, 5, 0.5, 0.05\}$. The mean time between collisions is 0.282.

Figure 5

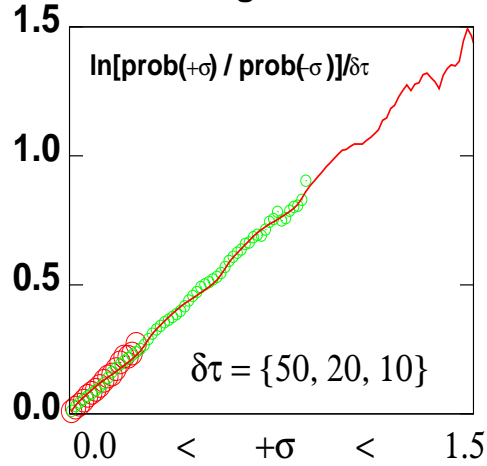


FIG. 5: $(1/\delta\tau) \ln[\text{prob}(+\sigma/k)/\text{prob}(-\sigma/k)]$ as a function of the entropy production rate σ/k averaged over intervals of length 10 (solid line), 20 (small open circles), and 50 (large open circles), corresponding to 36, 71, and 178 collision times. These data were accumulated from a 12-digit periodic orbit. According to the “Fluctuation Theorem” the slope of this curve is unity for sufficiently long averaging intervals. Generating and analyzing these data required just over a month of machine time. Boltzmann’s constant k is set equal to unity in the plot.

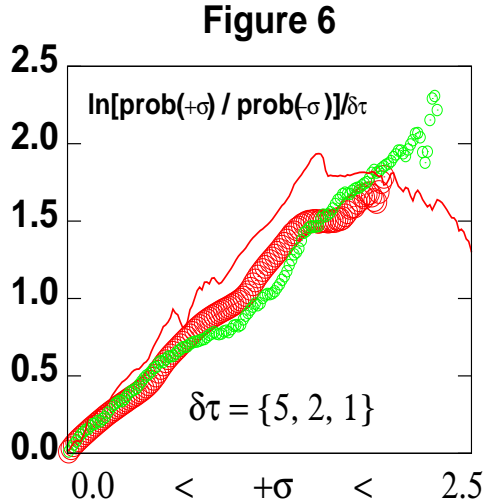


FIG. 6: $(1/\delta\tau) \ln[\text{prob}(+\sigma/k)/\text{prob}(-\sigma/k)]$ as a function of the entropy production rate σ/k averaged over intervals of length 1 (solid line), 2 (small open circles), and 5 (large open circles), corresponding to 4, 7, and 18 collision times. These data were accumulated from a 12-digit periodic orbit. According to the “Fluctuation Theorem” the slope of this curve is unity for sufficiently long averaging intervals. Generating and analyzing these data required just over a month of machine time. Boltzmann’s constant k is set equal to unity in the plot.

V. SUMMARY

The Fluctuation Theorem provides accurate estimates for the relative probability of forward and reversed steady-state phase-space trajectories. The Theorem illustrates the usefulness of coarse-grained probability densities in microscopic interpretations of macroscopic thermodynamics. Results for short-term nonequilibrium fluctuations (most of the data in Figure 4) are highly model dependent, and still lack accurate theoretically-based estimates.

The Fluctuation Theorem looks very much like Onsager’s (or Gibbs’) relation for probabilities in terms of a nonequilibrium phase-space entropy,

$$\text{prob} \simeq e^{\Delta S/k},$$

even though the nonequilibrium entropy does not exist^{1,7,19–21} outside the linear-response regime.

The Fluctuation Theorem goes beyond the Central Limit Theorem (which also applies to nonequilibrium steady states) and so can be used to give an explicit prediction for the halfwidth of the large- $\delta\tau$ Gaussian distribution:

$$\ln\left[\frac{\text{prob}(+\sigma)}{\text{prob}(-\sigma)}\right]_{FT} = \delta\tau\sigma/k \simeq \ln\left[\frac{\text{prob}(+\sigma)}{\text{prob}(-\sigma)}\right]_{CLT} = 2\sigma\langle\sigma\rangle/\Sigma^2 ,$$

where Σ is the standard deviation, and accordingly should be $\sqrt{2k\langle\sigma\rangle/\delta\tau}$. The two Theorems taken together do provide a useful semiquantitative guide to nonequilibrium fluctuations far from the linear-response regime.

The relationship between the length of coarse-grained periodic orbits and the multifractal correlation dimension can be derived from a statistical viewpoint, by imagining random jumps among N phase space states, resulting in an orbit length somewhat less than \sqrt{N} . In the present work the “jump” from one collision to the next can be viewed as such a process.

Many generalizations of this simple isokinetic model have been elaborated in the literature. By adding a magnetic field⁴ the time-reversibility of the equations of motion can be eliminated, but with the results still obeying the Fluctuation Theorem. A Nosé-Hoover thermostat⁵ allows for fluctuations in the kinetic energy, but without affecting reversibility. In both these cases the Fluctuation Theorem is obeyed for sufficiently large times. Results in the short-time limit, instantaneous fluctuations in the entropy production rate, are more highly model dependent and still cannot be predicted theoretically.

VI. ACKNOWLEDGMENTS

Thomas Gilbert and David Jou kindly provided us with advice and useful references, including a .pdf copy of Thomas’ 15/03/2006 seminar talk, “Fluctuation Theorem, A Selective Review and Some Recent Results”, and David’s contribution “Temperature, Entropy, and Second Law Beyond Local Equilibrium, an Illustration” to the Proceedings of the 2010 Granada Seminar in La Herradura. Christoph Dellago provided a copy of Reference 20 and Denis Evans made some useful comments on the first draft of this work. We thank Lakshmi Narayanan at World Scientific Publishers for her continuing support.

-
- ¹ Wm. G. Hoover, *Computer Simulation, Time Reversibility, and Chaos* (World Scientific Publishing, Singapore, 1999 and 2001).
 - ² D. J. Evans, E. G. D. Cohen, and G. P. Morriss, “Probability of Second Law Violations in Shearing Steady States”, *Physical Review Letters* **71**, 2401-2404 and 3616 (1993).
 - ³ E. G. D. Cohen and G. Gallavotti, “Note on Two Theorems in Nonequilibrium Statistical Mechanics”, *Journal of Statistical Physics* **96**, 1343-1349 (1999).
 - ⁴ M. Dolowschiák and A. Kovaács, “Fluctuation Formula for NonReversible Dynamics in the Thermostated Lorentz Gas”, *Physical Review E* **66**, 066217 (2002).
 - ⁵ M. Dolowschiák and A. Kovaács, “Fluctuation Formula in the Nosé-Hoover Thermostated Lorentz Gas”, *Physical Review E* **71**, 025202 (2005).
 - ⁶ T. Gilbert, “Fluctuation Theorem Applied to the Nosé-Hoover Thermostated Lorentz Gas”, *Physical Review E* **73**, 035102 (2006).
 - ⁷ B. Moran, W. G. Hoover, and S. Bestiale, “Diffusion in a Periodic Lorentz Gas”, *Journal of Statistical Physics* **48**, 709-726 (1987).
 - ⁸ F. Barra and T. Gilbert, “Nonequilibrium Lorentz Gas on a Curved Space”, *Journal of Statistical Mechanics*, L01003 (2007).
 - ⁹ C. Grebogi, E. Ott, and J. A. Yorke, “Roundoff-Induced Periodicity and the Correlation Dimension of Chaotic Attractors”, *Physical Review A* **38**, 3688-3692 (1988).
 - ¹⁰ C. Dellago and Wm. G. Hoover, “Finite-Precision Stationary States At and Away from Equilibrium”, *Physical Review E* **62**, 6275-6281 (2000).
 - ¹¹ Ch. Dellago, H. A. Posch, and W. G. Hoover, “Lyapunov Instability in a System of Hard Disks in Equilibrium and Nonequilibrium Steady States”, *Physical Review E* **53**, 1485-1501 (1996).
 - ¹² C. Grebogi, E. Ott, and J. A. Yorke, “Unstable Periodic Orbits and the Dimensions of Multifractal Chaotic Attractors”, *Physical Review A* **37**, 1711-1724 (1988).
 - ¹³ W. N. Vance, “Unstable Periodic Orbits and Transport Properties of Nonequilibrium Steady States”, *Physical Review Letters* **69**, 1356-1359 (1992).
 - ¹⁴ J. Machta and R. W. Zwanzig, “Diffusion in a Periodic Lorentz Gas”, *Physical Review Letters* **50**, 1959-1962 (1983).
 - ¹⁵ D. J. Evans and D. Searles, “The Fluctuation Theorem”, *Advances in Physics* **51**, 1529-1585

- (2002).
- ¹⁶ G. Benettin, L. Galgani, A. Giorgilli, J. M. Strelcyn, “Lyapunov Characteristic Exponents for Smooth Dynamical Systems and for Hamiltonian Systems, a Method for Computing All of Them”, *Meccanica* **15**, 9-20(1980).
 - ¹⁷ W. G. Hoover and H. A. Posch, “Direct Measurement of Equilibrium and Nonequilibrium Lyapunov Spectra” *Physics Letters A* **123**, 227-230 (1987).
 - ¹⁸ I. Goldhirsch, P.-L. Sulem, and S. A. Orszag, “Stability and Lyapunov Stability of Dynamical Systems: a Differential Approach and a Numerical Method”, *Physica* **27D**, 311-337 (1987).
 - ¹⁹ W. G. Hoover and B. Moran, “Phase-Space Singularities in Atomistic Planar Diffusive Flow”, *Physical Review A* **40**, 5319-5326 (1989).
 - ²⁰ C. Dellago, “Lyapunov Instability of Two-Dimensional ManyBody Systems”, *Doktor der Naturwissenschaften Dissertation* (Universität Wien, Wien, 1995).
 - ²¹ M. Criado-Sancho and J. E. Llebot, “Behavior of Entropy in Hyperbolic Heat Conduction”, *Physical Review E* **47**, 4104-4107 (1993).
 - ²² R. Klages, *Microscopic Chaos, Fractals, and Transport in Nonequilibrium Statistical Mechanics* (World Scientific Publishing, Singapore, 2007).
 - ²³ L. Rondoni and C. Mejía-Monasterio, “Fluctuations in Nonequilibrium Statistical Mechanics: Models, Mathematical Theory, Physical Mechanisms”, *Nonlinearity* **20**, R1-R37 (2007).